

Model for Ferromagnetic Quantum Critical Point in a 1D Kondo Lattice

Yashar Komijani¹ and Piers Coleman^{1,2}

¹*Department of Physics and Astronomy, Rutgers University, Piscataway, New Jersey, 08854, USA*

²*Department of Physics, Royal Holloway, University of London, Egham, Surrey TW20 0EX, UK*

(Dated: July 17, 2018)

Motivated by recent experiments, we study a quasi-one dimensional model of a Kondo lattice with Ferromagnetic coupling between the spins. Using bosonization and dynamical large- N techniques we establish the presence of a Fermi liquid and a magnetic phase separated by a local quantum critical point, governed by the Kondo breakdown picture. Thermodynamic properties are studied and a gapless charged mode at the quantum critical point is highlighted.

Heavy fermion materials are a class of quantum system in which the close competition between magnetism and itineracy drives a wealth of novel quantum ground states, including hidden order, strange and quantum critical metals, topological insulators and unconventional superconductivity [1, 2]. The various entanglement mechanisms by which the localized magnetic moments correlate and transform heavy fermion materials provide an invaluable window on the governing principles needed to control and manipulate quantum matter.

An aspect of particular interest is the quantum criticality that develops when a second-order magnetic phase transition is tuned to absolute zero. In weakly interacting materials, magnetic quantum phase transitions are understood in terms of the classic Slater-Stoner instabilities of Fermi liquids (FLs), described by the interaction of soft magnons with a Fermi surface according to the Hertz-Millis-Moriya theory [3–5]. The nature of quantum criticality in strongly interacting materials, in which the magnetism has a localized moment character, is less well understood, but is thought to involve a partial or complete Mott localization of the electrons, manifested in heavy fermion compounds as a break-down of the Kondo effect and a possible collapse in the Fermi surface volume [6–9].

Most research into heavy fermion quantum criticality has focused on antiferromagnetic instabilities, often discussed as a competition between the Kondo screening of local moments, and antiferromagnetism, driven by the Ruderman-Kittel-Kasuya-Yosida (RKKY) interaction [10–12]. However, there is now a growing family of heavy-fermion systems, including α and β -YbAlB₄ [13–15], YbNi₄P₂ [16], YbNi₃Al₉ [17] and CeRu₂Al₂B [18], in which the interplay of the Kondo effect and ferromagnetism is involved in the quantum criticality [19], including engineered chains of quantum dots on metallic surfaces [20, 21] and itinerant systems [22].

Motivated by these discoveries here we examine quantum criticality in a Kondo lattice with ferromagnetic interactions. This affords many simplifications, for the uniform magnetization M commutes with the Hamiltonian $[M, H] = 0$ and is thus a conserved quantity, free from quantum zero-point motion. Antiferromagnetic Kondo lattices are normally discussed in terms of a “global” phase diagram [6, 8] with two axes - the Doniach parameter $x = T_K/J_H$, set by the ratio of the Kondo temperature T_K to the Heisenberg coupling J_H , and the frustration parameter y measuring the strength of

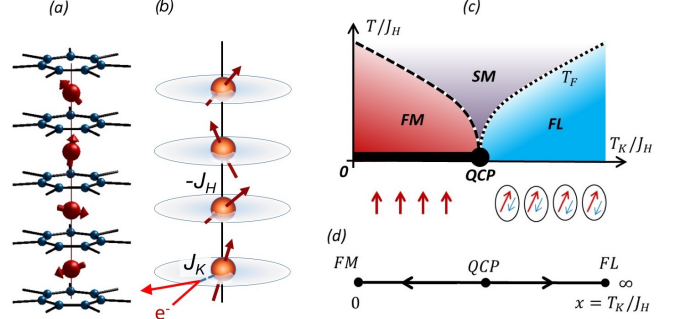


FIG. 1. (a) The quasi-1D structure of Yb local moments (red) in YbAlB₄ sandwiched between conducting B layers. (b) 1D model, showing local moments (orange), coupled via a ferromagnetic coupling $-J_H < 0$, each Kondo-coupled to a separate conduction electron sea (white-blue layers). (c) Phase diagram we find for the model as a function of T_K/J_H and temperature, showing Fermi liquid and 1D ferromagnetic regime, separated by a QCP. The Fermi temperature of the FL, T_F vanishes at the QCP. The 1D FM only orders at zero temperature and is intrinsically quantum critical. (d) RG flow of transverse Ising model to which our model maps in the Ising limit.

magnetic zero point fluctuations. The elimination of magnetic zero point fluctuations allows us to focus purely on the x -axis of the global phase diagram. Moreover, it now becomes possible to study magnetic quantum criticality in a one dimensional model.

Our model is motivated by the quasi-one dimensional Yb structure of YbAlB₄, in which a chain of ferromagnetically coupled Yb spins hybridizes with multiple conducting planes of B atoms (Fig. 1.) [23]. For simplicity, we treat each plane as an autonomous electron bath, individually coupled via an antiferromagnetic Kondo coupling J_K , according to

$$H = \sum_j \left(H_c(j) + J_K \vec{S}_j \cdot \vec{\sigma}_j - J_H \vec{S}_j \cdot \vec{S}_{j+1} \right), \quad (1)$$

where \vec{S}_j is the spin at the j -th site, coupled ferromagnetically to its neighbor with strength J_H . $H_c(j) = \sum_{\mathbf{p}} \epsilon_{\mathbf{p}} c_{\mathbf{p}\alpha}^\dagger(j) c_{\mathbf{p}\alpha}(j)$ describes the j -th layer of electrons, coupled to the chain via its spin density $\vec{\sigma}_j = \psi_{j\alpha}^\dagger \vec{\sigma}_{\alpha\beta} \psi_{j\beta}$ at the chain, where \mathbf{p} is the momentum of the conduction electrons at the j -th layer and $\psi_{j\alpha}^\dagger = \sum_{\mathbf{p}} c_{\mathbf{p}\alpha}^\dagger(j)$ creates an elec-

tron at the position of impurity site on the chain.

At small $x = T_K/J_H$ the 1D chain is ferromagnetically correlated, developing true long range order only at zero temperature, while at large x it forms a paramagnet where each spin is individually screened: in between, there is a quantum critical point (QCP) [10, 19]. This QCP has been demonstrated [21] in the Ising limit of this Kondo lattice at the Toulouse decoupling point [24, 25], which permits bosonization of the Hamiltonian, mapping it [26] onto the transverse field Ising model, $H \rightarrow T_K \sum_n S_n^x + J_H^z \sum_n S_n^z S_{n+1}^z$. This model has a well-known RG flow [Fig.1(d)] and a quantum phase transition at $J_H^z = T_K$ [27]. However, in this limit, the stable phases are gapped and to gain a deeper insight into the physics of the QCP, we return to the Heisenberg limit.

Here instead, we use a large- N Schwinger boson approach which treats the magnetism in the Heisenberg limit, while also explicitly preserving the Kondo effect. Our method unifies the Arovass and Auerbach treatment of ferromagnetism [28] with the description of the Kondo problem by Parcollet, Georges et al [29–32]. An important aspects of this approach, is the use of a multi-channel Kondo lattice in which the spin S and the number of channels K is commensurate ($K = 2S$), allowing for a perfectly screened Kondo effect [32].

Figure 1(c) summarizes the key results. At large T_K/J_H our method describes a FL phase with Pauli susceptibility $\chi \sim 1/T_F$ and a linear specific heat coefficient $\gamma = C/T \sim 1/T_F$. As x is reduced to a critical value x_c , the characteristic scale $T_F(x)$, determined from the magnetic susceptibility and linear specific heat coefficient (Fig. 2 (c,d)), drops continuously to zero, terminating at a QCP. This suppression of T_F resembles the Schrieffer mechanism for the reduction of the Kondo temperature in Hund's metals [33–36]. The large N QCP is characterized by powerlaw dependences of the specific heat, local and uniform susceptibilities.

$$\chi(T) \sim \frac{1}{T}, \quad \chi_{loc}(T) \sim \frac{1}{T^{1-\alpha}}, \quad \frac{C}{T} \sim \frac{1}{T^\alpha} \quad (2)$$

where the exponent $\alpha[s] < 1$ is function of the spin $s = 2S/N$. At still smaller x the chain develops a fragile Ferromagnetism which disappears at finite temperatures. Here $\chi \sim 1/T^2$ and $C/T \sim 1/\sqrt{T}$ characteristics of a critical 1D Ferromagnetism (FM). There are two notable aspects of the physics: first, the QCP exhibits an emergent critical charge fluctuation mode associated with Kondo breakdown, and secondly the 1D ferromagnetic ground-state is intrinsically quantum critical, transforming into a Fermi liquid with characteristic scale of order the Zeeman coupling, upon application of a magnetic field. This last feature is strongly reminiscent of the observed physics of β -YbAlB₄, a point we return to later.

Our large N approach is obtained by casting the local moments as Schwinger bosons $S(j)_{\alpha\beta} = b_{j\alpha}^\dagger b_{j\beta}$, where $2S = n_b(j)$ is the number of bosons per site, each individually coupled to a K channel conduction sea, with Hamiltonian

$$H = \sum_j [H_{FM}(j) + H_K(j) + H_C(j) + \lambda_j(n_b(j) - 2S)], \quad (3)$$

where (scaling down coupling constants)

$$\begin{aligned} H_{FM}(j) &= -(J_H/N)(b_{j\alpha}^\dagger b_{j+1,\alpha})(b_{j+1,\beta}^\dagger b_{j\beta}) \\ H_K(j) &= -(J_K/N)(b_{j\alpha}^\dagger \psi_{ja\alpha})(\psi_{ja\beta}^\dagger b_{j\beta}) \\ H_C(j) &= \sum_{\mathbf{p}} \epsilon_{\mathbf{p}} c_{\mathbf{p}a\alpha}^\dagger(j) c_{\mathbf{p}a\alpha}(j), \end{aligned} \quad (4)$$

where λ_j is a Lagrange multiplier that imposes the constraint. Here we have adopted a summation convention, with implicit summations over the (greek) $\alpha \in [1, N]$ spin and (roman) $a \in [1, K]$ channel indices. In the calculations, we take $2S = K = sN$ for perfect screening, where s is kept fixed.

Next, we carry out the Hubbard-Stratonovich transformations:

$$\begin{aligned} H_K(j) &\rightarrow [(b_{j\alpha}^\dagger \psi_{ja\alpha})\chi_{ja} + \text{h.c.}] + \frac{N\bar{\chi}_{ja}\chi_{ja}}{J_K} \\ H_{FM}(j) &\rightarrow [\bar{\Delta}_j(b_{j+1,\alpha}^\dagger b_{j,\alpha}) + \text{h.c.}] + \frac{N|\Delta_j|^2}{J_H}. \end{aligned} \quad (5)$$

The first line is the Parcollet-Georges factorization of the Kondo interaction, where the χ_{ja} are charged, spinless Grassman fields that mediate the Kondo effect in channel a . The second line is the Arovass-Auerbach factorization of the magnetic interaction in terms of the bond variables Δ_j describing the spinon delocalization. Both b and χ fields have non-trivial dynamics [29–32], with self-energies given by [37]

$$\Sigma_\chi(\tau) = g_0(-\tau)G_B(\tau), \quad \Sigma_B(\tau) = -kg_0(\tau)G_\chi(\tau). \quad (6)$$

Here $G_\chi(\tau)$, $G_B(\tau)$ and $g(\tau)$ are the local propagators of the holons, spinons and conduction electrons, respectively. The conduction electron self-energy is of order $O(1/N)$ and is neglected in the large- N limit, so that $g_0(\tau)$ is the bare local conduction electron propagator. The holon Green's function is purely local, given by $G_\chi(z) = [-J^{-1} - \Sigma_\chi(z)]^{-1}$, but the interesting new feature of our calculation is the delocalization of the spinons along the chain. Seeking uniform solutions where $\Delta_j = -\Delta$ and $\lambda_j = \lambda$, the spinons develop a dispersion $\epsilon_B(p) = -2\Delta \cos p$, with propagator $G_B(p, z) = [z - \epsilon_B(p) - \lambda - \Sigma_B(z)]^{-1}$. The momentum-summed *local* propagator is then

$$G_B(z) = \sum_p G_B(p, z) = \int \frac{d\epsilon_B \rho(\epsilon_B)}{z - \lambda - \epsilon_B - \Sigma_B(z)} \quad (7)$$

where $\rho(\epsilon_B) = (2\pi\Delta)^{-1}[1 - (\epsilon_B/2\Delta)^2]^{-1/2}$ is the bare spinon density of states. Using Cauchy's theorem,

$$G_B(z) = \frac{1}{\Omega[z]} \frac{1}{\sqrt{1 - [\Omega(z)/2\Delta]^2}} \quad (8)$$

where $\Omega(z) \equiv z - \lambda - \Sigma_B(z)$ [37].

Stationarity of the Free energy with respect to λ and Δ then leads to two saddle-point equations

$$\int_{-\infty}^{+\infty} \frac{d\omega}{\pi} n_B(\omega) \text{Im} [G_B(\omega - i\eta)] = s, \quad (9)$$

$$\frac{1 + \zeta \frac{\Delta^2}{J_H^2}}{J_H} = \int \frac{d\omega}{2\pi\Delta^2} n_B(\omega) \text{Im} [\Omega(z)G_B(z)]_{z=\omega+i\eta} \quad (10)$$

which determine λ and J_H self-consistently.

In (10) we have added an additional $\zeta \frac{\Delta^2}{J_H^2}$ which stabilizes the quantum critical point. Schwinger boson mean-field theories suffer from weak first order phase transitions upon development of finite Δ , due to fluctuation-induced attractive quartic $O(\Delta^4)$ terms in the effective action. This difficulty [38], has thwarted the study of quantum criticality with this method. These first order transitions are actually a non-universal artifact of the way the large N limit is taken, easily circumvented by adding a small repulsive biquadratic term $H'(j) = \zeta J_H (\vec{S}_j \cdot \vec{S}_{j+1})^2$ to the Hamiltonian. For an $SU(2)$ $S = 1/2$ moment, the biquadratic term can be absorbed into the Heisenberg interaction, but for the higher spin representations of the large N expansion, it contributes a positive quartic correction $O(\zeta\Delta^4)$ to the effective action that restores the second-order phase transitions (at both zero and finite temperature) to the large N limit [37]. In practice, a $\zeta \sim 0.001$ is sufficient to remove the first order transition, so that Δ tunes linearly with J_H across the quantum critical point.

To find $G_B(\omega)$ and $G_\chi(\omega)$ we solve Eqs.(6-9) self-consistently on a linear and logarithmic grid. The entropy formula from [31, 32] was used to compute the specific heat associated with these solutions [37].

In the Kondo limit ($T_K/J_H \gg 1$) the local moments are fully screened, forming a Fermi liquid; in the Schwinger boson scheme, the formation of Kondo-singlets is manifested as a spectral gap $\Delta_g \sim T_K$ [32] in the spectrum of the spinons and holons, where $T_K = f(T_K^0, s)$ and $T_K^0 = De^{-1/\rho J}$ is the Kondo temperature (Fig. 2(a)). The opening of this gap effectively confines the spinon and conduction electron into a singlet bound state, leaving behind an elastic resonant scattering potential which satisfies the Friedel sum rule with phase shift $\delta = \pi/N$.

In the opposite ferromagnetic limit $T_K/J_H \ll 1$, the chain forms a fragile ferromagnet. In this case, the spinons are condensed in the ground-state, but at finite temperatures, the spinon band is gapped: the constraint (9) ensures that the gap in the spectrum grows quadratically, $\Delta_b(T) \propto T^2$, and together with the quadratic dispersion, this leads to a free energy $F \propto T^{3/2}$, a critical susceptibility $\chi \propto T^{-2}$ and a specific heat coefficient $C/T \propto T^{-1/2}$ [28, 37], in agreement with Bethe ansatz [39–42]. The van-Hove singularity of density of states means that the ferromagnet is fragile, so that the bosons only condense, developing true long-range order at absolute zero.

Fig. 2 shows the evolution of properties between these two limits. As x is reduced, the spectral gap responsible for Fermi liquid behavior shrinks linearly to zero at the QCP at $x_c \approx 2$, an indication of Kondo break-down. This suppression of the Kondo temperature with x is closely analogous to reduction of the Kondo temperature by Hund's coupling [33, 36, 43], with $\Delta \sim J_H$ playing the role of the Hund's coupling and the ratio ξ/a of the spin correlation length to the lattice spacing,

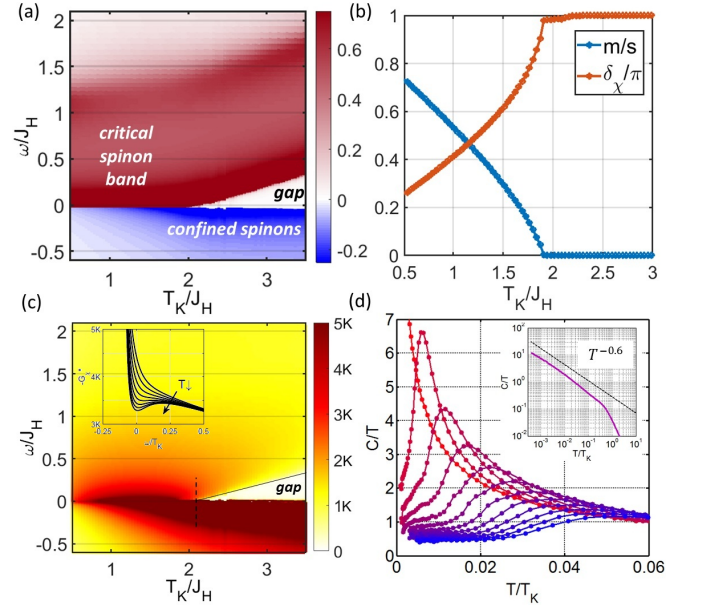


FIG. 2. (a) The spectral density of spinons $-G_B''(\omega + i\eta)$ for $k = s = 0.3$ as a function of T_K/J_H , shows spinon band at positive energy and the Kondo-screened spins appearing as confined spinons at negative energy. The Kondo gap at large x , shrinks linearly with lowering x , collapsing at about $x \approx 2$. (b) Zero temperature magnetization m/s (blue) and holon phase shift δ_χ/π (red) as a function of T_K/J_H . (c) The spectral density of holons $-G_\chi''(\omega + i\eta)$ as a function of T_K/J_H shows the Kondo-gap collapse and the critical mode at the QCP (inset). (d) specific heat coefficient $\gamma(T) = C/T$ vs. temperature as T_K/J_H is varied from 5 (blue) to 0.1 (red). The inset in (d) shows the power law dependence of γ at the QCP.

playing the role of the effective moment.

The ground-state ferromagnetic moment is given by

$$m = \lim_{T \rightarrow 0} \int_0^\infty \frac{d\omega}{\pi} n_B(\omega) \text{Im} G_B(\omega - i\eta). \quad (11)$$

which measures the residual positive-energy spinon population, which condenses at $T = 0$ (Fig. 2(b)). m is zero in the fully screened state, and rises gradually to a maximum value $m = s = 2S/N$ in the ferromagnetic limit. Note that $m/s < 1$ indicates that the magnetic moment is partially screened by an incipient Kondo effect which continues into the fragile magnetic phase.

Although our simple model does not allow us to examine the evolution of the Fermi surface, we can monitor the delocalization of heavy electrons by examining the phase shift of the holons $\delta_\chi = \text{Im} \ln[-G_\chi^{-1}(0 - i\delta)]$. The change in the number of delocalized heavy electrons Δn_f is related to the holon phase shift by the relation $\Delta n_f = \sum_a (\frac{\delta_\chi}{\pi})$ [31, 32], which is plotted as a function of x in Fig. 2(b). Although we do not observe a jump in Δn_f at the QCP, there is a sharp cusp in its evolution at $x = x_c$. One of the interesting aspects of our results, is that the holon spectrum becomes critical at the QCP (Fig. 2(c), inset), signaling the emergence of a critical spinless charge fluctuation that accompanies the critical formation and destruction of singlets.

The specific heat coefficient $\gamma \equiv C/T = dS/dT$, plotted in Fig. 2(d) shows a ‘‘Schottky’’ peak at $T \sim T_F$ for large x (blue) which collapses to zero as $x \rightarrow x_c$ (red). At the QCP, $\gamma(T) \sim T^{-\alpha}$ follows a power-law, where $\alpha[s]$ depends on the reduced spin $s = 2S/N$. In the calculations displayed here, $\alpha = 0.6$ for $s = 0.3$ (Fig. 2 d). In the magnetic phase $\gamma \sim 1/\sqrt{T}$ again characteristic of 1D FM.

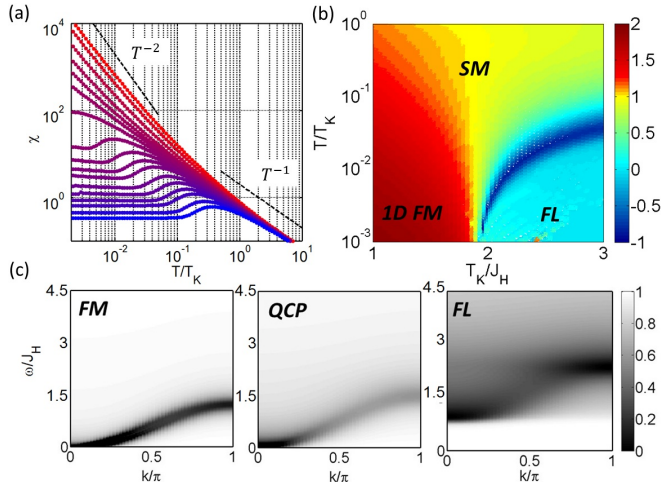


FIG. 3. (a) Uniform spin susceptibility χ as a function of temperature as T_K/J_H is varied from 0.1 (red) to 5 (blue). (b) The phase diagram obtained from the temperature-exponent κ of susceptibility $\chi \sim T^{-\kappa}$, shows the Kondo breakdown induced by the Schrieffer suppression of the Fermi temperature and separated from the magnetic phase by a QCP. (c) Dynamical spin susceptibility in FL ($T_K/J_H = 3.6$), QCP (1.65) and FM (0.36) regimes, respectively.

Fig. 3(a) shows the dependence of the uniform spin susceptibility on x . In the Fermi liquid at large x (blue), there is a cross over from a Curie susceptibility $\chi \sim 1/T$ at high- T to a Pauli susceptibility $\chi \sim 1/T_F$ at the Fermi temperature T_F . As x decreases, T_F decreases to zero and the susceptibility becomes critical. At the QCP the susceptibility $\chi \sim 1/T$ follows a simple Curie law. For $x < x_c$, the susceptibility displays a $\chi \sim 1/T^2$ characteristic of 1D FM. We use the dependence of the temperature exponent $\kappa = -d \log \chi / d \log T$ of the susceptibility on x and temperature to map out the phase diagram (Fig. 3(b)). The dark blue stripe delineates the renormalized Fermi temperature of the Fermi liquid, showing its collapse to zero as $x \rightarrow x_c^+$. The corresponding evolution in the dynamical magnetic susceptibility $\chi''(q, \omega)$ of various phases are shown in Fig. 3(c). The sharp magnon band in the magnetic phase is smeared at the QCP, denoting fractionalization of the spins. The FL phase features a spectral gap, which is an artifact of large- N method, as well as some remnants of the magnon band.

We have also studied the effect of a magnetic field [37]. While the Fermi liquid is robust, application of a small magnetic field to the QCP or the FM phase [44, 45] immediately reinstates Fermi-liquid behavior with a scale T_B set by the Zeeman energy (at the QCP) or a combination of the spinon bandwidth and magnetic field (in the FM phase) [37]. The

ferromagnetic phase is thus intrinsically quantum critical.

There are two interesting possibilities arising from our work; The intrinsic quantum criticality of the 1D FM phase is reminiscent of β -YbAlB₄. This raises the fascinating question as to whether the critical FM seen in our model might be stabilized by frustration, as a phase in higher dimensions. Second concerns the character of the Kondo break-down at the QCP, which appears to involve a critical spinless charge degree of freedom. It is intriguing to speculate whether this might be an essential element of a future theory of heavy fermion quantum criticality.

A natural extension of our work is the anti-ferromagnetism, which allows an exploration of the global phase diagram. Generalizations to higher dimensional systems can be envisioned by using our approach as an impurity or cluster solver for dynamical mean-field theory [46].

ACKNOWLEDGEMENT

This work was supported by a Rutgers University Materials Theory postdoctoral fellowship (YK), and by NSF grant DMR-1309929 (PC). We gratefully acknowledge discussions with Thomas Ayrar, Collin Broholm, Elio König, Satoru Nakatsuji, and Pedro Schlottmann.

- [1] F. Steglich and S. Wirth, *Reports on progress in physics. Physical Society (Great Britain)* **79**, 084502 (2016).
- [2] P. Coleman, *Introduction to Many-Body Physics* (Cambridge University Press, 2015).
- [3] J. A. Hertz, *Phys. Rev. B* **14**, 1165 (1976).
- [4] A. J. Millis, *Phys. Rev. B* **48**, 7183 (1993).
- [5] T. Moriya and T. Takimoto, *Journal of the Physical Society of Japan* **64**, 960 (1995).
- [6] Q. Si, S. Rabello, K. Ingersent, and J. L. Smith, *Nature* **413**, 804 (2001).
- [7] T. Senthil, S. Sachdev, and M. Vojta, *Phys. Rev. Lett.* **90**, 216403 (2003).
- [8] P. Coleman and A. H. Nevidomskyy, *Journal of Low Temperature Physics* **161**, 182 (2010).
- [9] Q. Si and F. Steglich, *Science* **329**, 1161 (2010).
- [10] S. Doniach, *Physica B+C* **91**, 231 (1977).
- [11] A. Schroder, G. Aeppli, R. Coldea, M. Adams, O. Stockert, H. Lohneysen, E. Bucher, R. Ramazashvili, and P. Coleman, *Nature* **407**, 351 (2000).
- [12] H. v. Löhneysen, A. Rosch, M. Vojta, and P. Wölfle, *Rev. Mod. Phys.* **79**, 1015 (2007).
- [13] S. Nakatsuji, K. Kuga, Y. Machida, T. Tayama, T. Sakakibara, Y. Karaki, H. Ishimoto, S. Yonezawa, Y. Maeno, E. Pearson, G. G. Lonzarich, L. Balicas, H. Lee, and Z. Fisk, *Nat Phys* **4**, 603 (2008).
- [14] Y. Matsumoto, S. Nakatsuji, K. Kuga, Y. Karaki, N. Horie, Y. Shimura, T. Sakakibara, A. H. Nevidomskyy, and P. Coleman, *Science* **331**, 316 (2011).
- [15] Y. Matsumoto, S. Nakatsuji, K. Kuga, Y. Karaki, Y. Shimura, T. Sakakibara, A. H. Nevidomskyy, and P. Coleman, *Journal of Physics: Conference Series* **391**, 012041 (2012).

- [16] A. Steppke, R. K uchler, S. Lausberg, E. Lengyel, L. Steinke, R. Borth, T. L uhmann, C. Krellner, M. Nicklas, C. Geibel, F. Steglich, and M. Brando, *Science* **339**, 933 (2013).
- [17] R. E. Baumbach, H. Chudo, H. Yasuoka, F. Ronning, E. D. Bauer, and J. D. Thompson, *Phys. Rev. B* **85**, 094422 (2012).
- [18] R. Miyazaki, Y. Aoki, R. Higashinaka, H. Sato, T. Yamashita, and S. Ohara, *Phys. Rev. B* **86**, 155106 (2012).
- [19] S. J. Yamamoto and Q. Si, *Proceedings of the National Academy of Sciences* **107**, 15704 (2010).
- [20] A. M. Lobos, M. A. Cazalilla, and P. Chudzinski, *Phys. Rev. B* **86**, 035455 (2012).
- [21] A. M. Lobos and M. A. Cazalilla, *Journal of Physics: Condensed Matter* **25**, 094008 (2013).
- [22] X. Y. Xu, K. Sun, Y. Schattner, E. Berg, and Z. Y. Meng, *Phys. Rev. X* **7**, 031058 (2017).
- [23] A. H. Nevidomskyy and P. Coleman, *Phys. Rev. Lett.* **102**, 077202 (2009).
- [24] G. Toulouse, *Comptes Rendu Academie Science* **268**, 1200 (1969).
- [25] V. J. Emery and S. Kivelson, *Phys. Rev. B* **46**, 10812 (1992).
- [26] Y. Komijani and P. Coleman, in preparation (2017).
- [27] S. Sachdev, *Quantum Phase Transitions*, 2nd ed. (Cambridge University Press, 2011).
- [28] D. P. Arovas and A. Auerbach, *Phys. Rev. B* **38**, 316 (1988).
- [29] O. Parcollet and A. Georges, *Phys. Rev. Lett.* **79**, 4665 (1997).
- [30] O. Parcollet, A. Georges, G. Kotliar, and A. Sengupta, *Phys. Rev. B* **58**, 3794 (1998).
- [31] P. Coleman, I. Paul, and J. Rech, *Phys. Rev. B* **72**, 094430 (2005).
- [32] J. Rech, P. Coleman, G. Zarand, and O. Parcollet, *Phys. Rev. Lett.* **96**, 016601 (2006).
- [33] J. R. Schrieffer, *Journal of Applied Physics* **38**, 1143 (1967).
- [34] A. I. Larkin and V. I. Mel'nikov, *Soviet Physics JETP* **34**, 656 (1972).
- [35] K. Haule and G. Kotliar, *New Journal of Physics* **11**, 025021 (2009).
- [36] A. H. Nevidomskyy and P. Coleman, *Phys. Rev. Lett.* **103**, 147205 (2009).
- [37] See supplementary material.
- [38] T. N. De Silva, M. Ma, and F. C. Zhang, *Phys. Rev. B* **66**, 104417 (2002).
- [39] P. Schlottmann, *Phys. Rev. Lett.* **54**, 2131 (1985).
- [40] P. Schlottmann, *Phys. Rev. B* **33**, 4880 (1986).
- [41] M. Takahashi and M. Yamada, *Journal of the Physical Society of Japan* **54**, 2808 (1985).
- [42] M. Takahashi, *Phys. Rev. Lett.* **58**, 168 (1987).
- [43] I. Okada and K. Yosida, *Progress of Theoretical Physics* **49**, 1483 (1973).
- [44] P. Coleman and C. P epin, *Phys. Rev. B* **68**, 220405 (2003).
- [45] P. Coleman and I. Paul, *Phys. Rev. B* **71**, 035111 (2005).
- [46] A. Georges, G. Kotliar, W. Krauth, and M. J. Rozenberg, *Rev. Mod. Phys.* **68**, 13 (1996).

SUPPLEMENTARY MATERIAL

Ferromagnetically coupled spin chain

Here, we briefly review the Arovas and Auerbach [28] treatment of 1D ferromagnetism. In absence of Kondo coupling, the Hamiltonian is $H_\lambda + H_{FM}$ where H_λ refers to the Lagrange multipliers. We assume a uniform mean-field solution Δ and find the temperature-dependence of the chemical potential.

Chemical potential - The number of bosons satisfies

$$s = \int_{-\pi}^{\pi} \frac{dk}{2\pi} n_B(\lambda + \epsilon_k) = \int d\epsilon \rho(\epsilon) n_B(\epsilon + \lambda), \quad (12)$$

When $T \ll \Delta$, the Bose Einstein function n_B is highly focused at low energies, and the physics is dominated by the quadratic bottom of the spinon band where $\epsilon_k = -2\Delta \cos k \approx -2\Delta + \Delta k^2$ so that

$$\rho(\epsilon) = \frac{2}{2\pi d\epsilon_k/dk} = \frac{1}{2\pi\Delta \sin k} \sim \frac{1}{2\pi\sqrt{\Delta}\sqrt{\epsilon + 2\Delta}}. \quad (13)$$

The factor of 2 in the numerator derives from the 2-to-1 relation between the momentum and energy ϵ_k . Using $\epsilon' = \epsilon + 2\Delta$ and $\lambda' = \lambda - 2\Delta$, we can write

$$\begin{aligned} s &= \frac{1}{2\pi\sqrt{\Delta}} \int_0^\infty d\epsilon' \frac{1}{\sqrt{\epsilon'}} \frac{1}{e^{\beta(\lambda' + \epsilon')} - 1} \\ &= \frac{1}{2\pi} \sqrt{\frac{T}{\Delta}} \Gamma(1/2) \text{Li}_{1/2}(z), \end{aligned} \quad (14)$$

where we have defined the fugacity $z \equiv e^{-\beta\lambda'}$ and used that

$$\begin{aligned} I_p(z) &\equiv \int_0^\infty dx \frac{x^{p-1}}{e^{x/z} - 1} \\ &= \sum_{k=0}^\infty \frac{z^{k+1}}{(k+1)^p} \int_0^\infty dy y^{p-1} e^{-y} \\ &= \Gamma(p) \text{Li}_p(z), \end{aligned} \quad (15)$$

in terms of polylogarithm function $\text{Li}_p(z)$. For $z = 1$ and $p > 1$ the series is convergent and $\text{Li}_p(z) = \zeta(p)$ where $\zeta(p)$ is the Riemann zeta function. But for $p < 1$ we also get convergence if $|z| < 1$. Due to the \sqrt{T} prefactor in the expression for s in Eq. (14), the function $\text{Li}_{1/2}(z)$ has to diverge as $T \rightarrow 0$ so that s stays constant and this happens for $z \rightarrow 1$ for which we have

$$\lim_{z \rightarrow 1} \text{Li}_{1/2}(z) = \frac{\sqrt{\pi}}{\sqrt{-\log(z)}} = \frac{\sqrt{\pi}}{\sqrt{\lambda'/T}}. \quad (16)$$

Therefore, we conclude

$$\lambda' = \alpha T^2, \quad \alpha = \frac{\Gamma^2(1/2)}{2\pi\Delta s^2}. \quad (17)$$

Δ vs. J_H - This can also be alternatively written as

$$\frac{\Delta}{J_H} = -\frac{1}{2\Delta} \int d\epsilon \epsilon \rho(\epsilon) n_B(\lambda + \epsilon) \quad (18)$$

Again assuming that the bottom of the band is only involved (this works in the limit of large Δ/T) we have

$$2\frac{\Delta^2}{J_H} = -\frac{1}{2\pi\sqrt{\Delta}} \int_0^\infty d\epsilon' \frac{\epsilon' - 2\Delta}{\sqrt{\epsilon'}} \frac{1}{e^{\beta(\epsilon' + \lambda')} - 1} \quad (19)$$

$$= -\frac{1}{2\pi\sqrt{\Delta}} \left[T\sqrt{T}I_{3/2}(z) - 2\Delta\sqrt{T}I_{1/2}(z) \right], \quad (20)$$

in terms of $I_p(z)$ defined in Eq. (15). Equivalently

$$\frac{2\Delta^{5/2}}{J_H} = -\frac{1}{2\pi} \left[T\sqrt{T}\Gamma(3/2)\text{Li}_{3/2}(z) - 2\sqrt{T}\Delta\Gamma(1/2)\text{Li}_{1/2}(z) \right]. \quad (21)$$

So, using $z\partial_z \text{Li}_p(z) = \text{Li}_{p-1}(z)$ we find

$$2\frac{\Delta^{5/2}}{J_H} = \frac{1}{2\pi} \left[2\Gamma(1/2) \times \sqrt{\pi} \frac{\Delta}{\sqrt{\alpha\Delta}} + T^2\sqrt{\alpha\Delta}2\sqrt{\pi}\Gamma(3/2) \right]. \quad (22)$$

At zero temperature, we can drop the second term in the right side and from $\alpha_\Delta \propto s^2/\Delta$ find

$$2\frac{\Delta^{5/2}}{J_H} = 2s\Delta^{3/2} \rightarrow \Delta(T \rightarrow 0) = J_H s. \quad (23)$$

Susceptibility - The susceptibility is

$$\begin{aligned} \chi &= -\frac{dM}{dB} \Big|_{B=0} = \frac{\beta}{L} \sum_k n_B(\lambda + \epsilon_k) [1 + n_B(\lambda + \epsilon_k)] \\ &= -\frac{1}{L} \sum_k \frac{-\beta e^{\beta(\lambda + \epsilon_k)}}{(e^{\beta(\lambda + \epsilon_k)} - 1)^2} \end{aligned} \quad (24)$$

Doing the momentum sum we find

$$\begin{aligned} \chi &= \beta \int \frac{dk}{2\pi} \frac{e^{\beta(\lambda + \epsilon_k)}}{[e^{\beta(\lambda + \epsilon_k)} - 1]^2} \\ &= \beta \int_0^\infty d\epsilon' \rho(\epsilon' - 2\Delta) \frac{e^{T\epsilon'/z}}{[e^{T\epsilon'/z} - 1]^2} \\ &= \frac{\beta}{4\pi\sqrt{\Delta}} \sqrt{T} \int_0^\infty dx \frac{1}{\sqrt{x}} \left\{ \frac{e^x/z}{[e^x/z - 1]^2} \right\} \\ &= \frac{T^{-1/2}}{4\pi\sqrt{\Delta}} \Gamma(1/2)\text{Li}_{-1/2}(z) \\ &\rightarrow \frac{\alpha^{-3/2}}{8\sqrt{\pi}\sqrt{\Delta}} \frac{1}{T^2}. \end{aligned} \quad (25)$$

where the last line is valid in the limit of low-temperature.

Free energy - This is simply

$$\begin{aligned} F + \lambda s &= \int \frac{d\omega}{\pi} n_B(\omega) \int d\epsilon \rho(\epsilon) \text{Im} [\log(\epsilon + \lambda - \omega - i\eta)] \\ &= \int \frac{d\omega}{\pi} \frac{n_B(\omega)}{2\pi\sqrt{\Delta}} \int_0^\infty \frac{d\epsilon'}{\sqrt{\epsilon'}} \text{Im} [\log(\epsilon' + \lambda' - \omega - i\eta)] \\ &= -\pi \frac{1}{2\pi\sqrt{\Delta}} \int \frac{d\omega}{\pi} n_B(\omega) \int_0^{\omega - \lambda'} \frac{d\tilde{\epsilon}}{\sqrt{\tilde{\epsilon}}} \\ &= -\pi \frac{1}{\pi\sqrt{\Delta}} \int \frac{d\omega}{\pi} n_B(\omega) \sqrt{\omega - \lambda'}. \end{aligned} \quad (26)$$

After a $\omega = \lambda' + Tx$ change of variable,

$$\begin{aligned} F &= -\lambda s - \frac{1}{\pi\Delta} T^{3/2} \int_0^\infty \frac{dx\sqrt{x}}{e^x/z - 1} \\ &= -2\Delta s - \lambda' s - \frac{T^{3/2}}{\pi\Delta} \Gamma(3/2)\text{Li}_{3/2}(z) \end{aligned} \quad (27)$$

The polylogarithm has the expansion

$$\text{Li}_{3/2}(z) = -2\sqrt{\pi \log(-z)} + \sum_{m=0} \frac{\log^m(z)\zeta(1/2 - m)}{m!}.$$

Inserting this and also Eq. (17) into Eq. (27),

$$\begin{aligned} F &= -2\Delta s - \frac{T^2\Gamma(1/2)}{2\pi\Delta s} [\Gamma(1/2) - 2\Gamma(3/2)] \\ &\quad - \frac{T^{3/2}}{\pi\sqrt{\Delta}} \Gamma(3/2)\zeta(1/2) + \dots \end{aligned} \quad (28)$$

Remarkably, the T^2 term is cancelled out due to $\partial_\lambda F = 0$ and the second line contributes a $F_T - F_0 \propto T^{3/2}$, giving a $S = -dF/dT \sim \sqrt{T}$ entropy and a $\gamma = C/T \propto 1/\sqrt{T}$ specific heat coefficient.

Dynamical large- N equations

We start from the Hamiltonian (2) in the paper. The interaction part of the action is

$$S_I = \frac{1}{\sqrt{N}} \sum_{j\alpha\alpha'} \int_0^\beta d\tau [\chi_{ja}(\tau) \bar{b}_{j\alpha}(\tau) \psi_{ja\alpha}(\tau) + \text{h.c.}] \quad (29)$$

First we integrate out the c -electron. The result is

$$S_I = \frac{1}{N} \sum_{j\alpha\alpha'} \int_0^\beta d\tau_1 d\tau_2 \left[\chi_{ja}(\tau_1) b_{j\alpha}^\dagger(\tau_1) g_0(\tau_1 - \tau_2) b_{j\alpha}(\tau_2) \chi_{ja}^\dagger(\tau_2) \right] \quad (30)$$

where $g_0(\tau)$ is the bare local conduction electron propagator. We decouple this by adding to the action a conjugate pair of two-point quantum fields

$$S' = N \int_0^\beta d\tau_1 d\tau_2 \hat{G}_B(\tau_2, \tau_1) \hat{\Sigma}_B(\tau_1, \tau_2) \quad (31)$$

by shifting

$$\begin{aligned} \hat{G}_B(\tau_2, \tau_1) &\rightarrow \hat{G}_B(\tau_2, \tau_1) + \frac{1}{N} \sum_{j\alpha} b_{j\alpha}^\dagger(\tau_1) b_{j\alpha}(\tau_2) \\ \hat{\Sigma}_B(\tau_1, \tau_2) &\rightarrow \hat{\Sigma}_B(\tau_1, \tau_2) + \frac{1}{N} g_0(\tau_1, \tau_2) \sum_{j\alpha} \chi_{ja}^\dagger(\tau_2) \chi_{ja}(\tau_1). \end{aligned}$$

we find

$$S' + S_I \rightarrow S' + \int_0^\beta d\tau_1 d\tau_2 \left[\sum_{n\alpha} b_{n\alpha}^\dagger(\tau_1) \hat{\Sigma}_B(\tau_1, \tau_2) b_{n\alpha}(\tau_2) + \sum_{nk} \chi_{nk}^\dagger(\tau_1) g_0(\tau_2, \tau_1) \hat{G}_B(\tau_1, \tau_2) \chi_{nk}(\tau_2) \right] \quad (32)$$

The free energy (the effective action times T) is

$$F[\hat{G}_B, \hat{\Sigma}_B] = NT \text{Tr} \log[\hat{\Sigma}_B(\tau_1, \tau_2) - G_{B0}^{-1}(\tau_1, \tau_2)] - N\lambda s - KTT \text{Tr} \log[g_0(\tau_2, \tau_1) \hat{G}_B(\tau_1, \tau_2) - G_{\chi 0}^{-1}(\tau_1, \tau_2)] + NT \int_0^\beta d\tau_1 d\tau_2 \hat{G}_B(\tau_2, \tau_1) \hat{\Sigma}_B(\tau_1, \tau_2) \quad (33)$$

where

$$G_{B0}^{-1}(\tau_1, \tau_2) = -(\partial_{\tau_1} + \lambda)\delta(\tau_1 - \tau_2) \quad (34)$$

$$G_{\chi 0}^{-1}(\tau_1, \tau_2) = -J_K^{-1}\delta(\tau_1 - \tau_2). \quad (35)$$

Here variables \hat{O} with a hat on them, are fluctuating variables that are integrated over inside the path integral. In the limit of large- N , we can carry out a mean-field treatment of the path integral by replacing it by its saddle-point value. Variation of the free energy w.r.t. Σ_B gives $[\Sigma_B - G_{B0}^{-1}]^{-1} + G_B = 0$, so G_B and Σ_B obey a Dyson equation. Before we carry out the variation w.r.t. G_B , it is convenient to define $\Sigma_\chi(\tau_1, \tau_2) \equiv g_0(\tau_2, \tau_1)G_B(\tau_1, \tau_2)$. If we furthermore define $G_\chi(\tau_1, \tau_2) = [G_{\chi 0}^{-1} - \Sigma_\chi]_{(\tau_1, \tau_2)}$, then variation of the free energy w.r.t. G_B gives

$$\Sigma_B(\tau_1, \tau_2) = -\gamma g_0(\tau_2, \tau_1)G_\chi(\tau_1, \tau_2) \quad (36)$$

These set of self-consistent equations have a time-translationally invariant solution, dependent only on the time difference $\tau_1 - \tau_2$.

We now show that these mean-field equations can be obtained from the saddle point of a Kadanoff-Baym free energy functional. By identifying the argument of first logarithm in (33) as G_B^{-1} , we rewrite the free energy as

$$(NL)^{-1}F[G_B] = T \text{Tr} \left\{ \log[-G_B^{-1}] + (G_{B0}^{-1} - G_B^{-1})G_B \right\} - \lambda s + f_3[G_B],$$

$$f_3[G_B] = -\gamma T \text{Tr} \log\{\Sigma_\chi[G_B] - G_{\chi 0}^{-1}\}$$

with $\Sigma_\chi[G_B] = g_0(\tau_2, \tau_1)G_B(\tau_1, \tau_2)$. If we take variations of this expression w.r.t. G_B , we recover expression (36). Next we elevate the free energy to a functional of G_χ and Σ_χ by rewriting f_3 as follows:

$$f_3[G_B] \rightarrow f_3[G_B, \Sigma_\chi, G_\chi]$$

$$= -\gamma T \text{Tr} \log[\Sigma_\chi - G_{\chi 0}^{-1}] - \gamma T \text{Tr} [\Sigma_\chi G_\chi]$$

$$+ \gamma T \text{Tr} [\Sigma_\chi[G_B] \times G_\chi].$$

Here, the last two terms basically cancel each other. If we set the variation of f_3 w.r.t. G_χ to zero, we recover $\Sigma_\chi = \Sigma_\chi[G_B]$. If we set the variation of f_3 w.r.t. Σ_χ to zero (only the

first two terms have to be taken into account) we find $G_\chi = [G_{\chi 0}^{-1} - \Sigma_\chi]^{-1}$ as we had above. Using the variation with respect to Σ_χ to get rid of Σ_χ in favor of G_χ , we find

$$f_3 = -\gamma T \text{Tr} \left\{ \log[-G_\chi^{-1}] + (G_{\chi 0}^{-1} - G_\chi^{-1})G_\chi \right\} + \gamma T \text{Tr} [\Sigma_\chi[G_B] \times G_\chi] \quad (37)$$

and this gives us final expression for the free energy in the form of a Luttinger-Ward functional of Green's functions

$$(NL)^{-1}F[G] = T \text{Tr} \left[\log(-G_B^{-1}) + (G_{B0}^{-1} - G_B^{-1})G_B \right] - \gamma T \text{Tr} \left[\log(-G_\chi^{-1}) - (G_{\chi 0}^{-1} - G_\chi^{-1})G_\chi \right] + T \mathcal{Y}[G_\chi, G_B] - \lambda s, \quad (38)$$

where

$$\mathcal{Y}[G_\chi, G_B] = \gamma \text{Tr} [\Sigma_\chi[G_B] \times G_\chi] \quad (39)$$

$$= \gamma \beta \int_0^\beta d\tau g_0(\tau) G_B(-\tau) G_\chi(\tau) \equiv \beta Y$$

or in real frequency

$$Y = \gamma \int \frac{d\omega_1}{\pi} \int \frac{d\omega_2}{\pi} f(\omega_1) f(\omega_2) G_\chi''(\omega_1) \text{Im} [g_0(\omega_2) G_B(\omega_1 + \omega_2)] - \gamma \int \frac{d\omega_1}{\pi} \int \frac{d\omega_2}{\pi} n_B(\omega_1) f(\omega_2) G_B''(\omega_1) \text{Im} [g_0(\omega_2) G_\chi^*(\omega_2 - \omega_1)].$$

The diagrammatic rationale for the self-energies (Eq.6 of manuscript) is shown in Fig. (4). Note that since $\delta F[G]/\delta G = 0$, the self-energies can be obtained from the Luttinger-Ward functional $\Sigma = \delta Y/\delta G$. $\Sigma_B(\tau) = -\gamma g_0(\tau)G_\chi(\tau)$ gives in real-frequency

$$\Sigma_B(\omega + i\eta) = \gamma \int_{-\infty}^{+\infty} \frac{d\omega'}{\pi} f(\omega') \left\{ g_c''(\omega') G_\chi^R(\omega - \omega') - g_c^R(\omega + \omega') G_\chi''(-\omega') \right\}, \quad (40)$$

and $\Sigma_\chi(\tau) = g_0(-\tau)G_B(\tau)$ gives in real-frequency

$$\Sigma_\chi^R(\omega + i\eta) = \int_{-\infty}^{+\infty} \frac{d\omega'}{\pi} \left[-G_B^R(\omega + \omega') f(\omega') g_c''(\omega') + G_B''(\omega') n_B(\omega') g_c(\omega' - \omega - i\eta) \right]. \quad (41)$$

To find self-consistent solution to the dynamical large- N equations, we have implemented Eqs. (40) and (41) on a linear and logarithmic frequency grid, iteratively, together with the corresponding Dyson's equations. We start at high-temperature and gradually reduce the temperature to have convergence.

Fig. (5) summarizes some aspects of the single-impurity Kondo physics as captured by the large- N approach [29].

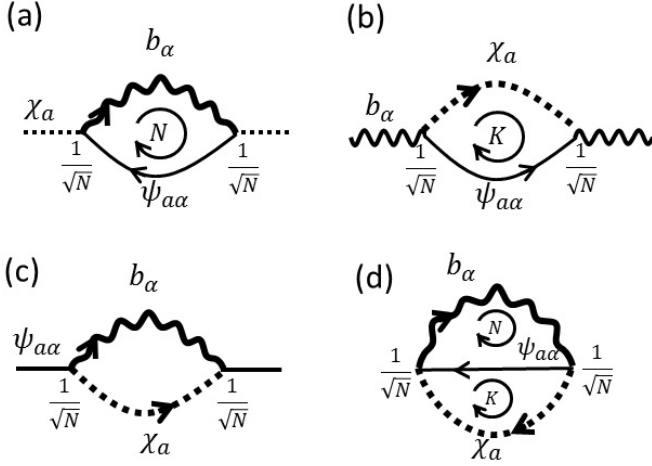


FIG. 4. (a-c) Diagrams for self-energy of (a) holon and (b) spinon and (c) the conduction electron. In two first two cases, the summation over the loop index (spin for holon and channel for boson) gives a factor of N which compensates $1/N$ coming from vertices, whereas no compensation in (c) means that conduction electron self-energy vanishes to $O(1)$ and corresponding Green's function remains bare. (d) The interaction part of the Luttinger-Ward functional. The self-energies can be obtained by cutting the corresponding propagator in this diagram $\Sigma = \delta Y / \delta G$.

Entropy

The free energy worked out in previous section is a stationary functional with respect to G_B , G_χ and λ . Keeping those constant, we take derivative w.r.t T to obtain the entropy. The result is [32]

$$S(T) = - \int \frac{d\omega}{\pi} \partial_T n_B(\omega) \left\{ \text{Im} \sum_k \log[-G_B^{-1}(k, \omega + i\eta)] + \Sigma_B''(\omega + i\eta) G_B'(\omega + i\eta) \right\} - k \int \frac{d\omega}{\pi} \partial_T f(\omega) \left\{ \text{Im} [\log[-G_\chi^{-1}(\omega + i\eta)]] + \Sigma_\chi''(\omega + i\eta) G_\chi'(\omega + i\eta) - g_0''(\omega + i\eta) \tilde{\Sigma}'_c(\omega + i\eta) \right\} \quad (42)$$

Here, g_0 is the bare Green's function of conduction band. And $\tilde{\Sigma}_c(\tau) = N \Sigma_c(\tau)$ where $\Sigma_c(\tau) = \frac{1}{N} G_B(\tau) G_\chi(-\tau)$ is the self-energy of the conduction electrons, which in the frequency domain is

$$\tilde{\Sigma}_c(\omega + i\eta) = \int \frac{d\nu}{\pi} \left[n_B(\omega) G_B''(\nu + i\eta) G_\chi(\nu - \omega - i\eta) - f(\nu) G_\chi''(\nu) G_B(\omega + \nu + i\eta) \right]. \quad (44)$$

At low temperature $\partial_T f(\omega) \propto \beta \omega \delta'(\omega)$ and as the fermionic functions do not diverge in the large- Δ limit, the residual entropy is dominated by the bosonic terms in the first two lines of Eq. (42).

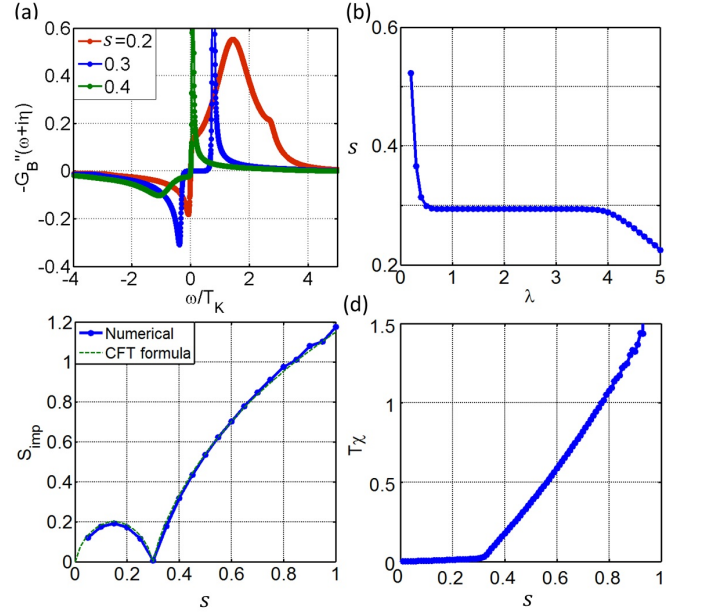


FIG. 5. The single-impurity multi-channel Kondo physics from the large- N approach. $k = 0.3$ is fixed and s is varied. (a) The spectrum of spinons for fully-screened (blue) over-screened (red) and under-screened (green) cases. (b) The gap in λ vs. s for establishing a Fermi-liquid. (c) Residual entropy and (d) T_χ as a function of s , which captures the Curie susceptibility coming from the residual un-screened moments.

Momentum sums

In this section we sketch the derivation of Eq. (8) and the expression used for the calculation of the spin susceptibility.

According to Cauchy's theorem,

$$F(z) = \oint \frac{dz'}{2\pi i} \frac{F(z')}{z' - z} = \int \frac{d\omega}{\pi} \frac{1}{\omega - z} \text{Im} [F(\omega + i\eta)] \quad (45)$$

where the contour in the first integral is counter-clockwise and in the second expression we have assumed that the the function $F(z')$ is analytical in the whole plane except on the real axis.

On the other hand for the local Green's function of the spinons we need to do the integral

$$G_B[\Omega(z)] = - \int \frac{d\epsilon_B \rho(\epsilon_B)}{\epsilon_B - \Omega(z)}, \quad \rho(\epsilon_B) = \frac{(2\pi\Delta)^{-1}}{\sqrt{1 - (\epsilon_B/2\Delta)^2}}.$$

where $\Omega(z) = z - \lambda - \Sigma_B(z)$. The function $\rho_B(\epsilon_B)$ can be expressed as the imaginary part of an analytical function

$$\rho(\epsilon_B) = -\text{Im} [F(\epsilon_B + i\eta)], \quad F(z) = \frac{1}{\pi z \sqrt{1 - (z/2\Delta)^{-2}}}.$$

Therefore, using (45), we find

$$G_B[\Omega(z)] = \frac{1}{\Omega \sqrt{1 - (\Omega/2\Delta)^{-2}}}. \quad (46)$$

The spin susceptibility can be expressed as the spinon bubble

$$\chi(k, \omega + i\eta) = \int \frac{dq}{2\pi} \int \frac{d\omega'}{\pi} n_B(\omega') G_B''(q, \omega') \quad (47)$$

$$[G_B(q + k, \omega' + \omega + i\eta) + G_B(q - k, \omega' - \omega - i\eta)].$$

For the static zero momentum case $k = \omega = 0$, we can write

$$\chi = \int \frac{d\omega}{\pi} n_B(\omega) \text{Im}[\chi_\omega], \quad \chi_\omega = \sum_k G_B^2(k, \omega + i\eta). \quad (48)$$

χ_ω can be expressed as the derivative of $G_B(z)$,

$$\chi_\omega = \int \frac{d\epsilon_B \rho(\epsilon_B)}{(\epsilon_B - \Omega)^2} = -\frac{d}{d\Omega} G_B(\omega + i\eta). \quad (49)$$

Therefore, we find

$$\chi_\omega = \frac{1}{\Omega^2 [1 - (\Omega/2\Delta)^{-2}]^{3/2}}. \quad (50)$$

For the bosonic contribution to the entropy we need

$$\mathcal{S}_\omega = \sum_k \log[-G_B^{-1}(k, \omega + i\eta)] = \int d\epsilon_B \rho(\epsilon_B) \log[\epsilon_B - \Omega].$$

Similar to above, \mathcal{S}_ω can be expressed as $\mathcal{S}_\omega \sim \int d\Omega G_B$. So,

$$\mathcal{S}_\omega = \log \left[1 + \sqrt{1 - (\Omega/2\Delta)^{-2}} \right] + \log(\Omega/2)$$

assuming $\text{Re}[\Omega/2\Delta] \leq -1$.

Applying magnetic field

We assume that the B -field couples to all but one boson b_1 increasing their energy, so that the field-dependent ‘‘Zeeman’’ term in the Hamiltonian takes the form

$$H_Z = B \sum_{\alpha \neq 1} b_\alpha^\dagger b_\alpha$$

For an isolated spin, this means that one of the bosons has the energy λ whereas the others have the energy $\lambda + B$. There are two phases [44, 45]: a paramagnetic phase at high temperature in which the population of the low-energy boson is negligible $\langle b_1 \rangle = 0$ and λ is adjusted so that $n_B(\lambda + B) = s$. Lowering the temperature λ decreases until it becomes zero at $T/B = 1/\log[1 + 1/s]$ below which the low-energy boson undergoes a Bose-Einstein condensation (BEC) $\langle b_1 \rangle^2 = s - n_B(B)$ to accommodate an $O(N)$ magnetization, the polarized phase. In presence of Kondo screening and the spinon hopping, essentially similar arguments apply except that the spinon energies are dressed by the hopping and renormalized by the spin fluctuations. We start by writing the Hamiltonian

in a magnetic field (L is the system size)

$$H = N \sum_{ja} \frac{\chi_{ja}^\dagger \chi_{ja}}{J_K} + \sum_{ja\alpha} (\chi_{ja} b_{ja\alpha}^\dagger \psi_{ja\alpha} + \text{h.c.}) \quad (51)$$

$$+ \lambda \sum_j [\sum_\alpha b_{j\alpha}^\dagger b_{j\alpha} - 2S] + B \sum_{j,\alpha \neq 1} b_{j\alpha}^\dagger b_{j\alpha} + H_C$$

$$- \Delta \sum_{j\alpha} [b_{j\alpha}^\dagger b_{j+1,\alpha} + \text{h.c.}] + N \frac{\Delta^2}{J_H}. \quad (52)$$

Separating the low-energy boson from the rest we have

$$H = N \sum_{ja} \frac{\chi_{ja}^\dagger \chi_{ja}}{J_K} + \sum_{ja,\alpha \neq 1} (\chi_{ja} b_{ja\alpha}^\dagger \psi_{ja\alpha} + \text{h.c.})$$

$$+ N \frac{\Delta^2}{J_H} - \Delta \sum_{j,\alpha \neq 1} [b_{j\alpha}^\dagger b_{j+1,\alpha} + \text{h.c.}]$$

$$+ (\lambda + B) \sum_j [\sum_{j,\alpha \neq 1} b_{j\alpha}^\dagger b_{j\alpha} - 2S] + 2SB + H_C$$

$$+ (\lambda - 2\Delta) \sum_j b_{j,1}^\dagger b_{j,1} + \sum_{ja} (b_{j,1}^\dagger \chi_{ja} \psi_{ja,1} + \text{h.c.}). \quad (53)$$

We consider a mean-field solution in which the low-energy boson condenses $b_1 \rightarrow \langle b_1 \rangle$. The condition for BEC is that the energy of b_1 boson becomes zero. But the apparent energy $\lambda - 2\Delta$ is further renormalized by the charge fluctuations in the last term. After the condensation, the Hamiltonian is (by $\chi \rightarrow \tilde{\chi}/\sqrt{N}$)

$$H = \sum_j \frac{\tilde{\chi}_{ja}^\dagger \tilde{\chi}_{ja}}{J_K} + \frac{1}{\sqrt{N}} \sum_{ja,\alpha \neq 1} (\tilde{\chi}_{ja} b_{ja\alpha}^\dagger \psi_{ja\alpha} + \text{h.c.})$$

$$- \Delta \sum_{n,\alpha \neq 1} [b_{n\alpha}^\dagger b_{n+1,\alpha} + \text{h.c.}] + N \frac{\Delta^2}{J_H} + H_C$$

$$+ N(\lambda + B) \left[\frac{1}{N} \sum_{\alpha \neq 1} b_\alpha^\dagger b_\alpha - q \right] + NBq$$

$$+ NL(\lambda - 2\Delta) \langle b_1 \rangle'^2 + \langle b_1 \rangle' \sum_{ja} (\tilde{\chi}_{ja} \psi_{ja,1} + \text{h.c.}) \quad (54)$$

Since, $\langle b_1 \rangle$ is extensive, we have defined $\langle b_1 \rangle' = \langle b_1 \rangle / \sqrt{N}$. As long as the $\langle b_1 \rangle' = 0$, λ adjusts itself so that the spectrum does not move. Also, note that once b_1 condenses in a magnetic field, the value of Δ might change, but for small B this is negligible and we have discarded the B -dependence of the mean-field Δ in this paper. To find the condensate fraction, we minimize the energy with respect to $\langle b_1 \rangle'$. So we find

$$(\lambda - 2\Delta) \bar{b}_1' = \frac{1}{NL} \sum_{ja} \text{Re} \langle \psi_{ja,1} \chi_{ja} \rangle \quad (55)$$

Considering that

$$\lim_{t \rightarrow 0} \langle \psi_{ja,1}(t) \chi_j(0) \rangle = i \int \frac{d\omega}{2\pi} G_{\psi\chi}^<(\omega), \quad (56)$$

and the relation

$$G_{\psi\chi}^<(\omega) = -f(\omega) [G_{\psi\chi}(\omega + i\eta) - G_{\psi\chi}(\omega - i\eta)], \quad (57)$$

we can write

$$(\lambda - 2\Delta)\bar{b}'_1 = \frac{1}{NL} \text{Re} \sum_j \lim_{t \rightarrow 0} \langle \psi_{ja,1}(t) \chi_{ja}(0) \rangle \quad (58)$$

$$= \gamma \int \frac{d\omega}{\pi} f(\omega) \text{Im} [G_{\psi\chi}(\omega + i\eta) - G_{\psi\chi}(\omega - i\eta)].$$

We can use equation of motion (EoM) to calculate the mixed function but first, better write $\psi_{ja,1}$ in momentum space:

$$G_{\psi\chi}(\tau) \equiv \langle -T c_{ja,1}(\tau) \chi_{ja} \rangle = \sum_k \langle -T c_{ja,1k}(\tau) \chi_{ja} \rangle. \quad (59)$$

Note that $c_{ja,1k}$ refers to $\alpha = 1$ and k is the electron momentum. EoM gives

$$\begin{aligned} -\partial_\tau G_{c\chi}(\tau) &= \langle -T [c_{ja1,k}, H]_\tau \chi_{ja} \rangle \\ &= \langle -T \{ \epsilon_k c_{ja1,k}(\tau) + \bar{b}'_1 \chi_{ja}^\dagger(\tau) \} \chi_{ja} \rangle, \end{aligned} \quad (60)$$

or

$$(-\partial_\tau - \epsilon_k) G_{c\chi}(\tau) = \bar{b}'_1 \langle -T \chi_{ja}^\dagger(\tau) \chi_{ja} \rangle, \quad (61)$$

which after momentum summation leads to

$$G_{\psi\chi}(\tau) = \bar{b}'_1 \sum_k g_k(\tau) * \langle -T \chi_{ja}^\dagger(\tau) \chi_{ja} \rangle. \quad (62)$$

To find the Fourier transform of the last term, note that fermionic Lehmann representation of $\langle -T \chi_j^\dagger(\tau) \chi_j \rangle$ is

$$G(i\omega_n) = -\frac{1}{Z} \sum_{mn} |\langle n | \chi | m \rangle|^2 \frac{e^{-\beta E_n} + e^{-\beta E_m}}{i\omega_n + E_n - E_m} \quad (63)$$

Therefore, $\chi \rightarrow \chi^\dagger$ corresponds to $n \leftrightarrow m$ and $G(i\omega_n) \rightarrow -G(-i\omega_n)$. So,

$$G_{\psi\chi}^R(\omega) = -\bar{b}'_1 g^R(\omega) G_\chi^A(-\omega). \quad (64)$$

Plugging this into Eq. (58) we find

$$\lambda - 2\Delta = -\gamma \int \frac{d\omega}{\pi} f(\omega) [g_{c1}''(\omega) G_\chi'(-\omega) - g_{c1}'(\omega) G_\chi''(-\omega)], \quad (65)$$

and of course $n_B(\lambda) = s - m$ where we defined the magnetization, $m \equiv \bar{b}'_1^2$. In the case of an isolated spin, it condensed

whenever its energy $\lambda = 0$ becomes zero. The above equation is generalization of that formula to the Kondo case. The self-energy of χ is modified

$$\Sigma_\chi(\tau) = \frac{N-1}{N} g_c(-\tau) G_{B,\alpha \neq 1}(\tau) - \bar{b}'_1^2 g_c(-\tau), \quad (66)$$

so that in large- N we have

$$\Sigma_\chi(\omega + i\eta) = \Sigma_\chi^{\text{old}}(\omega + i\eta) - m g_c(-\omega - i\eta) \quad (67)$$

and the self-energy of the bosons is not modified.

Thermodynamical properties in presence of magnetic field

We have computed the spin susceptibility and specific heat in presence of a magnetic field using the modification discussed in last section. The result is shown in Fig. (6). The Fermi liquid is robust against a magnetic field, and a field produces small quadratic shifts in the various mean-field quantities. However, in the gapless phases, application of a small magnetic field [44, 45] has a profound effect: it reinstates Fermi-liquid behavior with a scale T_B set by the Zeeman energy (at the QCP) or a combination of the spinon bandwidth and magnetic field (in the FM phase).

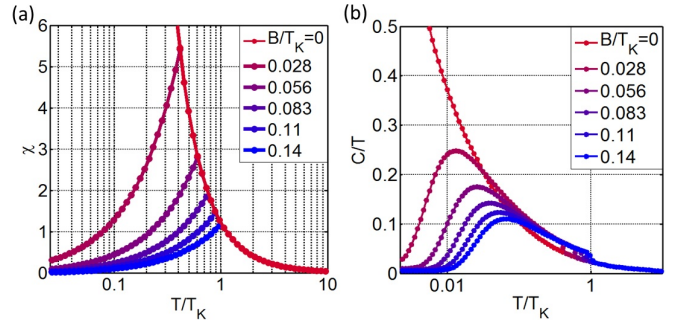


FIG. 6. Application of a magnetic field at $T_K/J_H = 0.1$ drives the (a) susceptibility χ and (b) specific heat coefficient γ from the critical behavior (red) to a FL behavior (blue). The kinks are due to a finite temperature FM transition induced by the field.